A UNIFIED BOUNDARY INTEGRAL EQUATION METHOD FOR A CLASS OF SECOND ORDER ELLIPTIC BOUNDARY VALUE PROBLEMS

M. REZAYAT, F. J. RIZZO and D. J. SHIPPY[1]

Abstract

A generalized integral equation formulation and a systematic numerical solution procedure are presented for a class of boundary value problems governed by a general second-order differential equation of elliptic type. Diverse numerical examples include problems of plane-wave scattering, three-dimensional fluid flow, and plane heat transfer for a body with a moving flame boundary. The last example employs certain representation functions useful to increase solution effectiveness in problems with an isolated integrable singularity.

1. Introduction

The partial differential equation

$$A_{\alpha\sigma}\frac{\partial^2\phi}{\partial x_\alpha \partial x_\sigma} + B_\alpha\frac{\partial\phi}{\partial x_\alpha} + C\phi = 0, \qquad \alpha, \sigma = 1, 2, \ldots, n, \tag{1.1}$$

in which $A_{\alpha\sigma}$, B_α and C are constants satisfying the ellipticity requirement (*cf.* [21]), may be reduced to the canonical form

$$\nabla^2\phi + \kappa\phi = 0 \tag{1.2}$$

where κ is a constant, $\phi = \phi(x_1, x_2, \ldots, x_n)$,

$$\nabla^2 \equiv \frac{\partial^2}{\partial x_1^2} + \frac{\partial^2}{\partial x_2^2} + \cdots + \frac{\partial^2}{\partial x_n^2} \tag{1.3}$$

---

[1] Department of Engineering Mechanics, University of Kentucky, Lexington, Kentucky 40506, U.S.A.

and, throughout this paper, summation is implied on repeated indices α and σ only. This differential equation, especially in the form (1.2), is the governing equation for a variety of boundary value problems which occur frequently in mathematical physics and engineering analysis. Specifically, if

$$\kappa \equiv k^2 \quad \text{with } k = \omega/c, n = 1, 2 \text{ or } 3 \tag{1.4}$$

where ω is a (real) frequency and c is a wave speed, then (1.2) is the "reduced" wave equation (or Helmholtz equation) governing time harmonic scalar wave propagation in a non-dissipative medium. Alternatively, with the choice

$$\kappa \equiv -\lambda^2, \qquad n = 2 \text{ or } 3 \tag{1.5}$$

(1.2) becomes a so-called "modified" Laplace equation which governs a variety of phenomena such as flame spread in a burning solid ([3], [7]) or flow of water in a leaky aquifer ([6], [10]). Also, (1.2) with (1.5) is identical with the Laplace transform of the classical scalar wave equation or the classical heat conduction equation under transient conditions, provided λ is identified (*e.g.* [15]) in terms of the transform parameter and relevant physical parameters. Finally, the choice $\kappa = 0$ reduces (1.2) to the ordinary Laplace equation.

Integral equation treatments of specific problems corresponding to particular choice of κ (*e.g.* [10], [15], [2], [12]) have been popular for some time for reasons of computational efficiency and accuracy (*cf.* remarks in [20], [16]). In most cases, however, formulations are tied closely to the particular problems at issue, and numerical techniques employed to solve the integral equations are varied, often elementary, and even crude by current standards. Further, while three-dimensional solutions exist (*e.g.* [12], [24]), the majority are limited to plane problems ($n = 2$).

The purpose of the present paper is first to view and formulate a Boundary Integral Equation (BIE) for all problems governed by (1.2) as a class. This BIE as obtained is valid for exterior and interior domains and for $n = 3$ as well as $n = 2$. Next, we describe a modern systematic process of numerical solution of the general BIE based on the use of "isoparametric" boundary elements. These elements are curvilinear triangles or quadrilaterals for $n = 3$ and curvilinear line elements for $n = 2$, for which the element geometry and the functions defined over the elements are represented as piecewise-quadratic polynomials. Further, for $n = 2$, we introduce certain "singular" shape functions which are useful when there is a singularity in one of the unknown boundary functions at certain points on the boundary of the relevant domain. Finally, we illustrate the entire BIE solution process with three numerical examples drawn from rather diverse physical situations. Specifically, we solve a plane-wave-scattering problem for $n = 2$ and a potential-flow problem for $n = 3$. Both problems involve potentials, one complex and the other real, defined in regions exterior to a simple, smooth, closed

surface. Such problems for exterior domains are particularly well suited to a BIE treatment, as opposed to field numerical methods, since only the boundaries need be discretized and conditions at infinity are easily handled analytically. The third example is a heat-conduction problem for $n = 2$ interior to a wedge-shaped domain, at one point of which there is an integrable singularity in heat flux. This problem, of some current practical importance [1], is solved for two values of the "wedge angle" using the mentioned singular shape functions. The latter provide for overall solution efficiency and accuracy of representation near the singularity.

2. BIE formulation

In the following, regard (1.2) as the governing differential equation for a sufficiently smooth function ϕ defined in a region B of two (E^2)- or three (E^3)-dimensional space with closed surface S. (While a BIE formulation for spaces E^n, $n > 3$, presents little difficulty, the numerical process to be described would be cumbersome, at best, to implement for such spaces, and we confine attention here to $n = 2$ and 3.) Next, let $K(x, y; \kappa)$ be the fundamental solution (*cf.* [8]) or free-space Green's function of (1.2), with the property

$$\nabla^2 K + \kappa K = \delta(x - y) \tag{2.1}$$

where $x \equiv (x_1, x_2)$ or (x_1, x_2, x_3), $y \equiv (y_1, y_2)$ or (y_1, y_2, y_3) are two points in B and $\delta(x - y)$ is the Dirac delta function. Now application of Green's theorem, with attention to the properties of the delta function (and an appropriate limit process as $x \in B \to x \in S$), leads (*cf.* [16]) to the integral expression

$$c(x)\phi(x) = \int_S [\phi(y)K_\nu(x, y; \kappa) - \phi_\nu(y)K(x, y; \kappa)] \, dS(y). \tag{2.2}$$

In (2.2) the subscript ν indicates the (outward) normal derivative of the function at $y \in S$, and the coefficient $c(x)$ has the values unity for $x \in B$ and zero for x in the region exterior to B. If $x \in S$, $c(x)$ may be obtained from (2.2) by choosing ϕ equal to a known elementary solution of (1.2). When a unique tangent (plane) exists at $x \in S$ it is easily shown that $c(x)$ equals one half. If B is the region exterior to a closed surface S, ϕ and ϕ_ν are assumed to behave, for indefinitely large y, such that the integrals in (2.2) taken over an indefinitely large sphere vanish (*cf.* [13], page 144). In general, S is assumed sufficiently regular (*cf.* [9]) to permit use of Green's theorem, and for $x \in S$ the integrals, though improper since K is singular for $y = x$, may be shown to exist.

Equation (2.2) may be regarded as an exact integral restatement of a boundary value problem governed by (1.2). Indeed, the BIE strategy for the solution of such problems is as follows. Place $x \in S$, determine $c(x)$, and prescribe (well posed)

parts of the function pair $\{\phi(y), \phi_\nu(y)\}$ on S; solve (2.2) for the unprescribed parts of that pair; place $x \in B$ and evaluate the (now known) integrals (2.2) to obtain the desired solution $\phi(x)$. Gradients of ϕ at $x \in B$ may be obtained by differentiation of the integrands in (2.2); note that only the known functions K and K_ν are affected, since they alone are functions of x on the right side of (2.2).

3. Numerical procedures

Since a strictly analytical process to carry out the described BIE strategy is out of the question for any practical problem, consider the following numerical solution procedure. Let S of B, $B \in E^3$, be discretized into a number M of curvilinear surface elements of either quadrilateral or triangular shape, and locate eight or six nodes, respectively, on each element. Half of the nodes are at the vertices and the other half are on the curvilinear edges of each element, the latter usually located midway between vertex nodes. The coordinates y_i^α of each node are specified, and the coordinates of a non-nodal point of an element are to be given by

$$y_i(\xi) = M^\alpha(\xi) y_i^\alpha, \qquad \alpha = 1, 2, \dots, 6 \text{ or } 8; \qquad i = 1, 2, 3, \qquad (3.1)$$

in which $M^\alpha(\xi)$ are second-order shape functions of intrinsic coordinates $(\xi) \equiv (\xi_1, \xi_2)$ of the type used in finite element analysis (see e.g. [25] and Appendix). The geometry of S is thus approximated by a system of piecewise-quadratic curvilinear elements coincident at the nodes. For $B \in E^2$, S is a curve or union of several curves, so that in (3.1) $\alpha = 1, 2, 3$; $i = 1, 2$; and ξ is a scalar variable. Next, assume that ϕ or ϕ_ν in (2.2) varies over the elements according to

$$\psi(\xi) = M^\alpha(\xi) \psi^\alpha \qquad (3.2)$$

where ψ^α is the nodal value of the variable at issue, so that ϕ and ϕ_ν are thus approximated by the same piecewise quadratic polynomials over the elements as those used to represent the geometry of the elements themselves. This is called an isoparametric representation.

Using this representation, (2.2) for $x \in S$ becomes

$$c(x_\beta)\phi(x_\beta) = \phi^{\alpha\sigma} \int_\gamma M^\alpha(\xi) K_\nu[x_\beta, y(\xi); \kappa] J^\sigma(\xi)\, d\xi$$

$$-\phi_\nu^{\alpha\sigma} \int_\gamma M^\alpha(\xi) K[x_\beta, y(\xi); \kappa] J^\sigma(\xi)\, d\xi \qquad (3.3)$$

in which $\sigma = 1, 2, \dots, M$ and $\beta = 1, 2, \dots, N$, where N is the total number of nodes. The quantities $\psi^{\alpha\sigma}$ mean "the value of ψ at local node α on surface element

S_σ", and $J^\sigma(\xi)$ is the ratio $dS_\sigma(y)/d\xi$ for the element S_σ. Note that (3.1) maps S_σ to the standard shape γ which is either a square or equilateral triangle in the space $\xi_1\xi_2$ for $B \in E^3$. For $B \in E^2$, γ is simply the interval -1 to 1.

The integrals in (3.3) involve only known integrands, and, although certain of them are improper when $x_\beta \in S_\sigma$, all are integrable either analytically or by Gaussian quadrature following removal of the singularity *via* transformation (see *e.g.* [16] or [17] for details). Then, adopting a global designation for $\psi^{\alpha\sigma}$ and letting x_β occupy all of the nodes, (3.3) may be viewed as a square $N \times N$ system of linear algebraic equations of the form

$$\mathbf{A}\phi = \mathbf{B}\phi_\nu, \tag{3.4}$$

in which the square matrices $\mathbf{A}$ and $\mathbf{B}$ contain the known integrals (and the $c(x_\beta)$ term) in (3.3). The columns ϕ and ϕ_ν contain the globally numbered nodal values of the original function pair $\{\phi, \phi_\nu\}$. Thus our solution strategy requires that $\mathbf{A}$ and $\mathbf{B}$ be calculated, an appropriate part of the pair $\{\phi, \phi_\nu\}$ be specified, and (3.4) be solved for the nonspecified part of that pair. Once this is done, an interior form of (3.3) is used to generate $\phi(x)$ pointwise at selected $x \in B$ to complete the solution process. Often, however, only the boundary solution is of interest, such that nonspecified ϕ or ϕ_ν or, perhaps, $d\phi/dS$ are all that are required. This last quantity is easily obtainable using the fact that $\phi(y)$ is represented in terms of ϕ and the shape functions.

In some problems, as is the case with the third of our example problems to follow, there is an integrable singularity in the first derivatives of ϕ (and thus in ϕ_ν) at one or more isolated points on the boundary S. In such a problem, representation of ϕ_ν by means of ordinary shape functions (*cf.* (3.2) and A.1) may be insufficient. Special shape functions are introduced in such a case as follows.
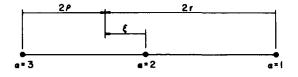

Figure 1. Standard boundary element in E^2.

Consider a standard element γ in E^2, with local nodes $\alpha = 1, 2, 3$ and intrinsic variable ξ as shown in Figure 1. Suppose the function $\phi_\nu(\xi)$ has a singularity at node 1 of known order s such that we may define a special shape function of the form

$$M_s^1(r) = Ar^s + Br^2 + Cr + D, \qquad 2r \equiv 1 + \xi \tag{3.5}$$

with the requirements that for

$$
\begin{aligned}
r \to 0, & \quad M_s^1(r) \to \infty, \\
r = \tfrac{1}{2}, & \quad M_s^1(r) = 0, \\
r = 1, & \quad M_s^1(r) = 0.
\end{aligned}
\tag{3.6}
$$

These requirements may be satisfied by choosing

$$
A = 1, \quad B = 4(\tfrac{1}{2})^s - 2, \quad C = 1 - 4(\tfrac{1}{2})^s, \quad D = 0
\tag{3.7}
$$

so that in terms of ξ, M_s^1 has the form

$$
M_s^1(\xi) = (\tfrac{1}{2})^s \big[(1 + \xi)^s - (1 - \xi^2)\big] - \tfrac{1}{2}\xi(1 + \xi).
\tag{3.8}
$$

Thus if $\phi_\nu(\xi)$ has a singularity of order s at node 1, then replacing $M^1(\xi)$ in (A.1) by $M_s^1(\xi)$ as given by (3.8) will result in a more accurate representation of $\phi_\nu(\xi)$ over γ. Note that the quantity ϕ_ν^1 in the representation $\phi_\nu(\xi) = M^\alpha(\xi)\phi_\nu^\alpha$ is no longer the value of ϕ_ν at node 1 under these circumstances. Rather, ϕ_ν^1 here is a finite-valued constant expressible in terms of the coefficient of the power of r representing the singularity (*e.g.* term in parenthesis in (6.7)).

With the introduction of $M_s^1(\xi)$, it is clear from (3.3) that it is now necessary to evaluate integrals of the form

$$
I^1 = \int_{-1}^1 M_s^1(\xi) K\big[x_\beta, y(\xi); \kappa\big] J^\sigma(\xi)\, d\xi
\tag{3.9}
$$

as ingredients in the matrix $\mathbf{A}$ of (6.12). The "singular" part of this integral is

$$
I_s^1 = \int_{-1}^1 (1 + \xi)^s K\big[x_\beta, y(\xi); \kappa\big] J^\sigma(\xi)\, d\xi
\tag{3.10}
$$

in which the singularity in K is logarithmic as $\xi \to x_\beta$. Four cases of interest occur: x_β occupies none of the nodes on γ, and $\beta = 1, 2, 3$, *i.e.* x_β at each of the three nodes on γ. For the first case, (3.10) may be integrated by parts, and for the range of s of interest in our third example (*cf.* (6.7) *et seq.*) the resulting integrand in the remaining integral is nonsingular and may be evaluated by Gaussian quadrature as usual. For x_β occupying the nodal positions, an integration by parts together with the transformations

$$
\begin{aligned}
\xi = 1 - \zeta^2, & \quad \alpha = 1, \\
\xi = \zeta^2 \text{ or } \xi = -\zeta^2, & \quad \alpha = 2, \\
\xi = \zeta^2 - 1, & \quad \alpha = 3,
\end{aligned}
\tag{3.11}
$$

again produces non-singular integrands. Transformations (3.11) are used according as x_β occupies the indicated positions (for $\alpha = 2$, $\xi = \zeta^2$ is used for integration from nodes 1 to 2 and $\xi = -\zeta^2$ for integration from nodes 2 to 3). Again, ordinary Gaussian quadrature may be used.

Modifications associated with a singular shape function $M_s^3(\xi)$ to be used if the singularity occurs at node 3 are almost identical to the above. By choosing an element endpoint (node 1 or 3) to coincide with a singularity, one need never be concerned with a shape function $M_s^2(\xi)$.

4. A plane-wave-scattering problem

Let a rigid circular cylinder of unit radius be surrounded by a scalar-wave-propagating medium B, of infinite extent, with wave-propagation speed c. Further, let ϕ be the (complex) velocity potential (*e.g.* [20]) for time-harmonic waves in B of frequency ω, such that

$$\nabla^2\phi + k^2\phi = 0 \qquad (4.1)$$

must hold throughout B, where the wave number $k \equiv \omega/c$. Moreover, we assume that ϕ satisfies the Sommerfeld radiation conditions ([13], page 144). Now let ϕ_0 be the potential for a plane harmonic wave incident on the cylinder such that the cylinder axis is parallel to the plane of the incident wave. We seek the total wave potential ϕ in B, which is the sum $\phi_0 + \phi_s$, where ϕ_s is the field scattered from the cylinder.
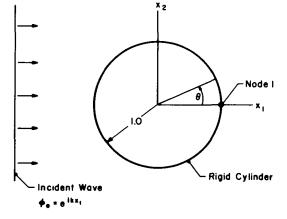

Figure 2. Plane wave scattering problem.

All variables in this problem, as posed, are independent of x_3, the direction of the cylinder axis, so that the problem becomes one in E^2. The circular boundary S, the coordinate system, and the incident wave are as shown in Figure 2. The necessary function K (*cf.* (2.1)) for (4.1) in E^2 is

$$K(x, y; k) = \tfrac{i}{4}[H_0(kr)], \qquad i = \sqrt{-1} \qquad (4.2)$$

with $r \equiv |y - x|$, and H_0 is the Hankel function of the first kind of order zero. Therefore, including the effects of ϕ_0 directly ($cf.$ [13]), (2.2) becomes explicitly

$$c(x)\phi(x) = \phi_0(x) + \frac{i}{4}\int_S\left[\phi(y)H_{0,\nu}(x, y; k) - \phi_\nu(y)H_0(x, y; k)\right]dS(y)$$

$$(4.3)$$

where $c(x)$ is 1 or $\frac{1}{2}$ according as $x \in B$ or $x \in S$, respectively. For the rigid cylinder, $\phi_\nu(y) = 0$, so that the second integral in (4.3) vanishes, and we seek $\phi(y)$.

Now, as discussed in Section 3, the approximate form of (4.3) is

$$\mathbf{A}\boldsymbol{\phi} = \boldsymbol{\phi}_0 \qquad (4.4)$$

in which ϕ and ϕ_0 are the nodal values of the unknown surface potential and the known incident plane-harmonic potential, respectively. The matrix $\mathbf{A}$ is as described in (3.4). Specifically, we first discretize the circle S into $M = 9$ equal-length curvilinear elements and $N = 18$ nodes, $i.e.$, a node is located on S
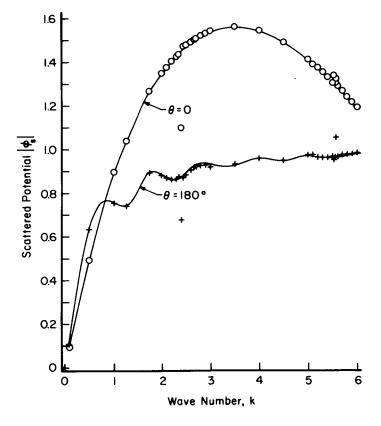

Figure 3. Scattered potential as a function of wave number.

at equal intervals of 20° beginning with node 1 on the x_1 axis. This discretization is used for all chosen values of k up to $k = 3.0$. For values of $k > 3.0$, $N = 36$ nodes is used, *i.e.* a node every 10° on S. Higher values of k require increased resolution for accuracy, as might be expected.

Data are obtained for nodes at $\theta = 0°$ and $\theta = 180°$, and the magnitude $|\phi_s| \equiv (\Re\phi_s^2 + \Im\phi_s^2)^{1/2}$ of the scattered potential is plotted in Figure 3 as a function of k for these two positions. The solid curve represents the analytical solutions, and the ($\circ$) and ($+$) represent the BIE data. Results as shown are excellent except for data in the vicinity of $k = 2.405$ and $k = 5.572$, which are wave numbers corresponding to eigenfrequencies of the "associated interior problem" under the soft ($\phi = 0$) boundary condition (*cf.* [5]). Inaccurate BIE data are expected at or very near these values of k, since any integral formula of the type (4.3) is known to break down at such wave numbers. It is possible to reformulate the scattering problem (*e.g.* [19], [11]) to circumvent the difficulties with the mentioned eigenfrequencies, but such reformulation is beside the purpose of the present paper. However, we find that with the present procedures, ordinary accuracy is obtainable at values of k which are two to three percent away from the eigenvalue, so that serious difficulty with this "fictitious eigenfrequency" phenomenon is not, in fact, encountered. Further, the reciprocal of the condition number of the matrix of coefficients **A** drops noticeably in size very near the eigenvalues. This could be used as a guide to the acceptability of computed data near an eigenvalue in problems where that eigenvalue may be *a priori* unknown.

5. A potential flow problem

To illustrate the solution process for a problem in E^3, consider the flow of an ideal fluid past a rigid sphere of radius a. For flow in the positive x_3 direction the well known expression (*e.g.* [18]) for the velocity potential ϕ is

$$\phi = U(1 + a^3/2R^3)R\cos\theta \qquad (5.1)$$

in which R is the distance from the sphere's centre to an arbitrary field point x, θ is the angle between R and the x_3 axis and U is the undisturbed or free-stream velocity. The potential ϕ satisfies Laplace's equation

$$\nabla^2\phi = 0 \qquad (5.2)$$

in the region B exterior to the spherical surface S, with $\phi_\nu = 0$ on S itself.

Now we seek a BIE solution for the function $\phi^* = \phi - UR\cos\theta$ where on s, $\phi_\nu^* = U(R/a)\cos\theta$. We choose to work with ϕ^* explicitly rather than ϕ, since ϕ^*

satisfies the required conditions at infinity whereas ϕ does not. The necessary function K (cf. (2.1)) for (5.2) in E^3 is

$$K(x, y) = 1/4\pi r(x, y) \qquad (5.3)$$

such that (2.2) explicitly becomes

$$c(x)\phi^*(x) = \frac{1}{4\pi} \int_S \left[\phi_\nu^*(y) \frac{1}{r(x, y)} - \phi^*(y) \left(\frac{1}{r(x, y)} \right)_\nu \right] dS(y) \qquad (5.4)$$

where again $r = |y - x|$, $c(x) = 1$ or $\frac{1}{2}$ according as $x \in B$ or $x \in S$, respectively, and in which we specify $\phi_\nu^* = U(R/a)\cos\theta$.

Under a discretization of S as discussed in Section 3 the approximate form of (5.4) may be written as

$$\mathbf{A}\phi^* = \mathbf{b}^* \qquad (5.5)$$

where $\mathbf{b}^* \equiv \mathbf{B}\phi_\nu^*$ is a known vector (cf (3.4)), and ϕ^* and ϕ_ν^* represent nodal values of the functions ϕ^* and ϕ_ν^*, as before. Here we consider two discretizations of the spherical surface S into curvilinear triangular elements. The first discretization divides S into octants, so that $M = 8$ elements with $N = 18$ nodes. The second discretization uses a symmetrical subdivision of each octant into three smaller, congruent, curvilinear triangular elements, such that $M = 24$ elements with $N = 50$ nodes. For each discretization ϕ^* is obtained as the solution of (5.5).

For the cruder discretization, ϕ^* departs from the corresponding analytical values by about 13%. At points $x \in B$ at distances from 1.5a to 100a, (5.4) (with $c(x) = 1$) yields ϕ^* values averaging 20% error. Using the finer discretization these errors are reduced to 3% and 4% respectively. Note that $M = 24$, though finer than $M = 8$, is still a somewhat crude discretization of a spherical surface. We find both sets of accuracy figures surprisingly good (cf. [12], [4] using plane triangle elements) and suggestive of the computational efficiency of the isoparametric representation for curved surfaces in three dimensions.

6. A moving-flame, heat-conduction problem

The following is a basic model for a class of problems in flame-spread analysis with application to fire control ([7], [1]). Consider an indefinitely long, infinitely wide slab of combustible solid material of finite thickness which is burning at one end. A typical plane section of the slab is shown in Figure 4a. The flame is confined to the inclined faces of the wedge-shaped end, and the burning process causes the wedge shape to move downward at a uniform speed V_F while the wedge angle α remains constant.
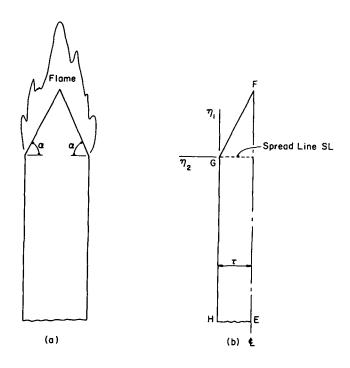
Figure 4. Burning slab model.

Allowing axes of spatial coordinates η_i $(i = 1, 2)$ to move with the flame, the governing differential equation in non-dimensional form for the thermal field throughout the slab (*e.g.* [1]) is

$$\nabla^2\theta = P\frac{\partial\theta}{\partial\eta_1}, \qquad \nabla^2 \equiv \frac{\partial^2}{\partial\eta_1^2} + \frac{\partial^2}{\partial\eta_2^2} \tag{6.1}$$

where θ is the non-dimensional temperature, and P is the so-called Péclet number. This number is known in terms of the slab half-thickness τ, V_F, and other thermal parameters. We need consider only a half-thickness of the slab as shown in Figure 4b, and from symmetry there is zero heat flow across the centre-line EF.

The specific boundary value problem here is to find θ throughout the finite plane region $EFGH$ under the boundary conditions

$$\begin{aligned} \theta_\nu &= 0 &&\text{on edges } EF, GH, \\ \theta &= 1 &&\text{on edge } FG, \\ \theta &= 0 &&\text{on edge } HE. \end{aligned} \tag{6.2}$$

Of particular interest in this problem is the heat flux Q across the spread line (SL), $i.e.$,

$$Q = \int_{SL} \frac{\partial \theta}{\partial \eta_1} d\eta_1 \equiv P \int_{SL} \theta \, d\eta_1 \tag{6.3}$$

where the second integral expression for Q follows from Green's theorem.

Now (6.1) can be easily put in the form (1.2) through the transformation

$$\theta = \exp(p\eta_1)\psi, \qquad P \equiv 2p \tag{6.4}$$

such that in terms of the transformation function ψ, (6.1) becomes

$$\nabla^2 \psi - p^2 \psi = 0 \tag{6.5}$$

with

$$
\begin{aligned}
\psi_\nu &= 0 &&\text{on edges } EF, GH, \\
\psi &= \exp(-p\eta_1) &&\text{on edges } FG, \\
\psi &= 0 &&\text{on edge } HE,
\end{aligned}
\tag{6.6}
$$

as the corresponding boundary conditions.

The boundary value problem in the form (6.5), (6.6) is now ready for a BIE treatment as in the preceding sections, but it should be noted that a singularity in the function ψ_ν exists at the point G for $\alpha > 0$ (Figure 4). An elementary eigenvalue analysis ($cf.$ [22], [23]) reveals that for sufficiently small r near G, we may obtain the order of singularity in ψ_ν from

$$\psi(r, \hat{\theta}) = r^\lambda \left(c_1 \sin \lambda\hat{\theta} + c_2 \cos \lambda\hat{\theta} \right), \tag{6.7}$$

where $(r, \hat{\theta})$ are polar coordinates of a point in B or S near G, c_1 and c_2 are constants, and λ has the value $\pi/2\beta$ with $\beta = \pi/2 + \alpha$ (Figure 4). Clearly then, ψ has an unbounded gradient for $\pi/2 < \beta < 2\pi$ at $r = 0$. Physically, this implies that the local heat flux q, which is proportional to ψ_ν at any boundary point, is undefined at G. This singularity, however, is integrable, so that while attention is required to represent this singularity with special shape functions ($cf.$ (3.5) $et\ seq.$) with attendant modifications in the numerical process, the analytical BIE statement of the problem may proceed as outlined in Section 2.

The necessary function K ($cf.$ (2.1)) for (6.5) in E^2 is

$$K(x, y; k) = \tfrac{1}{2\pi} K_0(x, y; p) \tag{6.8}$$

where K_0 is the modified Bessel function of the second kind of order zero. The BIE formula, $i.e.$ (2.2), now has the explicit form

$$2\pi c(x)\psi(x) = \int_S \left[\psi_\nu(y) K_0(x, y; p) - \psi(y) K_{0_\nu}(x, y; p) \right] dS(y) \tag{6.9}$$

where S is the boundary of the region in Figure 4b, *i.e.* the union of the line segments *EFGH*. Here $c(x) = 1$ for $x \in B$, where B is the region interior to S, and $c(x) = \frac{1}{2}$ for $x \in S$, except when x occupies the "corner" points, E, F, G, and H. At these points $c(x)$ equals the interior angle (in radians). However, $c(x)$ for any $x \in S$ may be obtained without explicit attention to the corner points, since the function

$$\psi^* \equiv \exp(p\eta_1) \tag{6.10}$$

is an elementary solution of (6.5) and thus satisfies (6.9) as well. Substituting ψ^* into (6.9) and solving for $c(x)$ we obtain

$$c(x) = \frac{1}{2\pi} \int_S \left\{ \frac{\exp(p\eta_1(y))}{\exp(p\eta_1(x))} \left[pK_0(x, y; p) - K_0(x, y; p) \right] \right\} dS(y) \tag{6.11}$$

which is used for all computations of $c(x)$, $x \in S$, including x at the corner points. This approach for $c(x)$ provides more systematic and accurate computation of improper integrals which arise following discretization of (6.9) than would separate calculation of interior angles at corners (*cf.* [15]).

In the present problem, boundary data (see (6.6)) are mixed such that the unknown functions in (6.9) are $\psi(y)$ on edges *EF* and *GH* and $\psi_\nu(y)$ on edges *FG* and *HE*. Under a discretization of S, (6.9) has the form
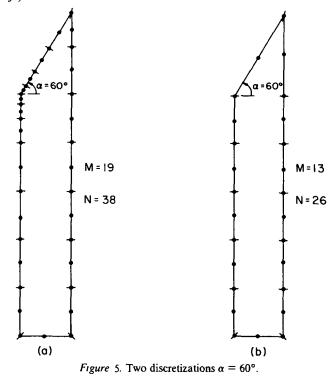
$$\mathbf{Au} = \mathbf{v} \tag{6.12}$$

in which $\mathbf{u}$ is the vector of unknown values of ψ and ψ_ν at nodes on S, except, of course, for the value of ψ_ν at point G, which is undefined. (See comment following (3.8).) Also $\mathbf{v}$ is the vector of known nodal values obtained from integrals of prescribed (non-zero) data, and $\mathbf{A}$ is the matrix of coefficients of the unknowns, as before. However, here $\mathbf{A}$ includes integrals of special shape functions used to represent ψ_ν over one element on S, adjacent to point G, at one end of which ψ_ν is singular. Using $\tau = 1$ and locating surface *HE* 5 units away from the spread line (Figure 4b) proved sufficient to employ the $\theta = 0$ ($\psi = 0$) boundary conditions on *HE* for all calculations.

For $\alpha = 0$, there is no singularity at point G, and the analytical solution in terms of θ with boundary conditions (6.2) is simply $\theta = \exp(p\eta_1)$. Using $M = 16$ elements ($N = 32$ nodes), BIE data for θ on the boundary and at several interior points compare with analytical values with an error of less than 0.1%. Normalized flux values, θ_ν, on S, similarly compare with an error of 0.15%.

For $0 < \alpha < \pi/2$ the situation is complicated by the fact that θ_ν is singular at point G with order of singularity $r^{\lambda-1}$ (see (6.7) *et seq.*), and an analytical solution is not available for data verification. The authors [1] were interested in the solution of this problem prior to the development of the singular shape functions

(SSF) as described in Section 3. It was decided to obtain BIE data, using ordinary shape functions (OSF) (A.1), for α in increments of $10°$ from $\alpha = 0°$ to $\alpha = 90°$, for a variety of Péclet numbers P. Sufficiently fine discretizations (large M with small elements "bunched" near G) were used to try to obtain meaningful values of Q (6.3) and θ (along edge GH), which were of primary interest in their heat transfer studies [1]. It was anticipated that the admitted inadequate representation of the singularity in θ_ν at G using OSF would be minimized with the fine "mesh" near G and that the variable of interest away from G would be little affected. By and large, this proved to be true; Q as a function of α obtained from the BIE analysis agreed well with asymptotic expressions valid for small α and/or large P. Further, surface θ so obtained agreed well with experimental values for $\alpha = 80°$ and several values of P as shown in detail in [1]. However, despite the success in [1] for the intended purpose there, we were dissatisfied with the "brute force" discretization procedures used and raised the following questions. To what extent could coarser discretizations be used with SSF and maintain desired accuracy of all data? Also, how well could we represent θ_ν along edge GF using SSF and how bad was the representation using OSF? (The criteria for mesh grading suggested in [14] would undoubtedly improve the performance of the OSF in representing the singularity.)
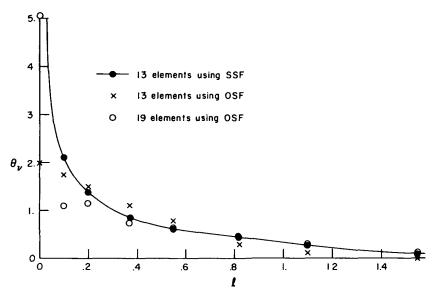

Figure 5. Two discretizations $\alpha = 60°$.

Figure 6. Behavior of θ_ν on edge GF near G.

To answer these questions, SSF were introduced as indicated in Section 3, and additional BIE solutions were obtained for the $\alpha = 60°$ and $\alpha = 80°$ cases, with $P = 1$, using successively coarser meshes and comparing accuracy and CPU times using OSF and SSF. It was found that a reduction of 20% to 30% in the total number of elements with no need for bunching of elements near G could be achieved using SSF, maintaining comparable accuracy of data overall. For example, Figure 5 depicts two discretizations for $\alpha = 60°$, the coarser of which yielded virtually identical Q and surface θ using SSF as did the finer one using OSF. CPU time, mostly dependent on M, was reduced accordingly. Moreover, when used with OSF the coarser mesh yielded data differing from the accepted values by as much as 7% away from the singularity (see Table 1).

Near the singularity, the variation of θ_ν with distance l from G along edge GF is depicted in Figure 6. The solid curve is the representation using SSF for the known order of singularity for $\alpha = 60°$. Clearly the representation using OSF is different very near G where the SSF representation approaches the exact representation. Thus through increased accuracy of local representation the SSF seem to provide a measure of overall computation efficiency as well.

Numerical data for the problems in this and the preceding sections were obtained using an IBM 370/165 computer with no advantage taken of any symmetry in B in programming. Execution times for individual problem solutions ranged from 2 to 15 seconds.

TABLE 1. The boundary temperature at $\eta_1 < 0$ and $\eta_2 = 0$ for $\alpha = 60°$ and Péclet number of one.

η_1 ($\eta_2 = 0$)	Boundary temperature θ		
	OSF Mesh Figure 5a	SSF Mesh Figure 5b	OSF Mesh Figure 5b
−0.5	0.4538	0.4579	0.4845
−1.0	0.2636	0.2663	0.2823
−1.5	0.1565	0.1581	0.1678
−2.0	0.0928	0.0937	0.0996
−2.5	0.0544	0.0549	0.0584
−3.0	0.0311	0.0314	0.0334
−3.5	0.0169	0.0171	0.0182
−4.0	0.0084	0.0084	0.0090
−4.5	0.0032	0.0032	0.0034

Acknowledgements

Appendix

Ordinary Shape Functions
(a) One-Dimensional (E^2)

$$M^1(\xi) = -\tfrac{1}{2}(\xi - \xi^2), \quad M^2(\xi) = 1 - \xi^2, \quad M^3(\xi) = \tfrac{1}{2}(\xi + \xi^2). \quad (A.1)$$

(b) Quadrilateral (E^3)

$$M_R^1(\xi) = \tfrac{1}{4}(\xi_1 + 1)(\xi_2 + 1)(\xi_1 + \xi_2 - 1), \quad M_R^5(\xi) = \tfrac{1}{2}(\xi_1 + 1)(1 - \xi_2^2),$$
$$M_R^2(\xi) = \tfrac{1}{4}(\xi_1 - 1)(\xi_2 + 1)(\xi_1 - \xi_2 + 1), \quad M_R^6(\xi) = \tfrac{1}{2}(\xi_2 + 1)(1 - \xi_1^2),$$
$$M_R^3(\xi) = \tfrac{1}{4}(1 - \xi_1)(\xi_2 - 1)(\xi_1 + \xi_2 + 1), \quad M_R^7(\xi) = \tfrac{1}{2}(\xi_1 - 1)(\xi_2^2 - 1),$$
$$M_R^4(\xi) = \tfrac{1}{4}(\xi_1 + 1)(\xi_2 - 1)(\xi_2 - \xi_1 + 1), \quad M_R^8(\xi) = \tfrac{1}{2}(1 - \xi_2)(1 - \xi_1^2).$$
$$(A.2)$$

(c) Triangular

$$M_T^1(\xi) = \xi_1(2\xi_1 - 1), \quad M_T^4(\xi) = 4\xi_1\xi_3,$$
$$M_T^2(\xi) = \xi_2(2\xi_2 - 1), \quad M_T^5(\xi) = 4\xi_1\xi_2, \quad \xi_1 + \xi_2 + \xi_3 = 1, \quad (A.3)$$
$$M_T^3(\xi) = \xi_3(2\xi_3 - 1), \quad M_T^6(\xi) = 4\xi_2\xi_3.$$

References

[1] R. A. Altenkirch, M. Rezayat, R. Eichhorn and F. J. Rizzo, "A study of heat conduction forward of flame spread in solids; by the boundary integral equation method", *Trans. ASME Ser. C J. Heat Transfer* 104 (1982), 734–740.

[2] R. P. Banaugh and W. Goldsmith, "Diffraction of steady acoustic waves by surfaces of arbitrary shape", *J. Acoust. Soc. Amer.* 35 (1963), 1590–1601.

[3] H. S. Carslaw and J. C. Jaeger, *Conduction of heat in solids* (Oxford University Press, London, 1967).

[4] L. H. Chen and D. G. Schweikert, "Sound radiation from an arbitrary body", *J. Acoust. Soc. Amer.* 35 (1963), 1626–1632.

[5] L. G. Copley, "Fundamental results concerning integral representations in acoustic radiation", *J. Acoust. Soc. Amer.* 44 (1968), 28–32.

[6] Roger J. M. DeWiest, "Flow to an eccentric well in a leaky circular aquifer with varied lateral replenishment", *Geofis. Pura Appl.* 54 (1963), 90–102.

[7] A. E. Frey and J. S. T'ien, "A theory of flame spread over a solid fuel including finite-rate chemical kinetics", *Combustion and Flame* 36 (1979), 263–289.

[8] F. John, *Plane waves and spherical means* (Interscience, New York, 1st edition, 1955).

[9] O. D. Kellogg, *Foundatins of potential theory* (Dover, New York, 1st edition, 1953).

[10] O. E. Lafe, "Boundary integral solutions to nearly horizontal flows in multiply zoned aquifers", Ph.D. Thesis, Cornell University, 1981.

[11] P. A. Martin, "On the null-field equations for the exterior problems of acoustics", *Quart. J. Mech. Appl. Math.* 33 (1980), 385–396.

[12] W. L. Meyer, W. A. Bell, B. T. Zinn and M. P. Stallybrass, "Boundary integral solutions of three dimensional acoustic radiation problems", *J. Sound and Vibration* 59 (1978), 245–262.

[13] Y. H. Pao and Ch. Ch. Mow, *Diffraction of elastic waves and dynamic stress concentrations* (Crane, Russak and Company Inc., New York, 1973).

[14] J. R. Rice, "On the degree of convergence of nonlinear spline approximation", in *Approximation with special emphasis on spline functions* (ed. I. J. Schoenberg), (Academic Press, New York, 1969).

[15] F. J. Rizzo and D. J. Shippy, "A method of solution for certain problems of transient heat conduction", *AIAA J.* 8 (1970), 2004–2009.

[16] F. J. Rizzo and D. J. Shippy, "The boundary integral equation method with application to certain stress concentration problems in elasticity", *J. Austral. Math. Soc. Ser. B* 22 (1981), 381–393.

[17] F. J. Rizzo and D. J. Shippy, "An advanced boundary integral equation method for three-dimensional thermoelasticity", *Internat. J. Numer. Methods Engrg.* 11 (1977), 1753–1768.

[18] H. Rouse (ed.), *Advanced mechanics of fluids* (John Wiley and Sons, Inc., New York, 1969).

[19] H. A. Schenck, "Improved integral formulation for acoustic radiation problems", *J. Acoust. Soc. Amer.* 44 (1968), 41–58.

[20] R. P. Shaw, "Boundary integral equation methods applied to wave problems", in *Developments in boundary element methods*-1, Chapter 6, 121–154.

[21] S. L. Sobolov, *Partial differential equations of mathematical physics* (Pergamon Press, London, 1964).

[22] M. Stern, "On calculating thermally induced stress singularities", *Conference on thermal stresses in severe environment* (Plenum Press, 1980), 123–134.

[23] M. L. Williams, "Stress singularities resulting from various boundary conditions in angular corners of plates in extension", *J. Appl. Mech.* 74 (1952), 526–528.

[24] Y. S. Wu, "The boundary integral equation method using various approximation techniques for problems governed by Laplace's equation", Master's thesis, University of Kentucky, 1976.

[25] O. C. Zienkiewicz, *The finite element method* (McGraw-Hill Book Company (UK) Limited, London, 3rd edition, 1977).